Proceedings of the 4th Jagiellonian Symposium on Advances in Particle Physics and Medicine

Positron Annihilation Spectroscopy of Oxygen Content Tissue-Equivalent Samples

M. Zare[a], O. Kakuee[b], B. Ghasemi[a] and A. Biganeh[b,*]

[a] *Nuclear engineering school, Shahid Beheshti University, Daneshjoo Blvd, Velenjak St., P.O. Box 1983969411, Tehran, Iran*
[b] *Physics & Accelerators Research School, Nuclear Science and Technology Research Institute, North Karegar st., P.O. Box 14395-836, Tehran, Iran*

Doi: 10.12693/APhysPolA.142.367 *e-mail: abiganeh@aeoi.org.ir

In this paper, the potential biomedical application of the positron annihilation spectroscopy for tumor imaging systems is investigated. The positron annihilation lifetime spectroscopy and coincidence Doppler broadening spectroscopy are performed for oxygen-content tissue-equivalent polymers to determine the oxygen sensing ability of positronium atoms for the detection of tissue hypoxia. The results of the coincidence Doppler broadening spectroscopy experiment confirmed that the measured momentum of the annihilated electrons varies in the presence of oxygen. The results of the positron annihilation lifetime spectroscopy showed that due to the quenching role of the oxygen in the positronium formation, the τ_3 and I_3 parameters are sensitive to the concentration of oxygen in the content. However, when the oxygen concentrations differ by less than 4%, factors such as chemical environments, nano-structures of the matter, free volumes, and areas around the molecule are the other main factors influencing the lifetime of the probes. So, using positronium as a biomarker for tissue hypoxia needs more data to support the technique.

topics: positron annihilation lifetime spectroscopy (PALS), positronium, tumor imaging, hypoxia

1. Introduction

Positron annihilation spectroscopy (PAS) is a well-established technique for the characterization of defects in metals, semiconductors, and polymers [1]. PAS includes coincidence Doppler broadening spectroscopy (CDBS) for investigation of the chemical environment of defects and positron annihilation lifetime spectroscopy (PALS) for exploring the size and density of defects [2]. Recently, the topic of the potential biomedical application of PAS has been raised. Moskal et al. [3] introduced a new concept for positronium (Ps) imaging of tumor cells named J-PET. This concept is based on the accepted hypothesis that the oxygen concentration in tumor tissue is less than in healthy tissue. The reason is the massive cell proliferation that distances cells from the vasculature. This condition in solid tumors is called tumor hypoxia and increases the patient's treatment resistance and contributes to tumor progression [4]. How hypoxic conditions are created in tumor tissues and how cells respond to hypoxia are fundamental questions in understanding tumor progression and metastasis. The possibility of determining the time and position of Ps annihilation for tumor imaging has been discussed by Moskal [5]. The feasibility study of the Ps imaging based on the Ps mean lifetime has been presented in [6]. The first Ps imaging of a phantom built from cardiac myxoma and adipose tissue, demonstrating the possibility of the PALS and PET, was obtained by the J-PET group at Jagiellonian University [7]. Their measurement was done by simultaneous registration of the annihilation of annihilation photons from pharmaceuticals labeled with radionuclide and adipose tissue. J-PET group has also demonstrated a tomographic reconstruction technique based on Ps decay into three photons [8]. The study on the parameters of the PAS that are related to the concentration of oxygen in the samples is of outstanding technical importance to designing a PET system based on Ps imaging. Experimental investigations show that Ps lifetime is different for healthy and tumor tissues [9]. However, due to the complicated history of the Ps atom, a combination of physical and chemical conditions in the tissue may be the origin of this difference. The main factors influencing the lifetime of probes are the chemical environment and nano-structure of matter, the occurrence of free volumes, and areas with reduced electron density. The challenging issue that should be addressed is how each factor changes the Ps lifetime. A limited number of experimental data is reported to clarify the effect of oxygen concentration on the Ps lifetime. Stepanov et al. [10] have shown a correlation between oxygen pressure (pO_2) and Ps lifetime in water. They also have developed the computer software "RooPositron" for analyzing lifetime

spectra according to the different mechanisms of Ps interactions [11]. Shibuya et al. [12] have compared the annihilation rates of Ps in O_2^-, N_2^-, and air-saturated waters. Their results confirm that Ps can probe the absolute value of pO_2 with good linearity and a resolution better than 10 mmHg.

Our approaches to dealing with the subject are as follows:

1. The sensitivity of the positron in the presence of oxygen in the tissue-equivalent polymers is investigated by CDBS.
2. The positron annihilation parameters related to the concentration of oxygen are explored using the PALS technique.

2. Theoretical details

For conventional PAS, the positron source is sandwiched between two identical samples. The emitted positrons penetrate the sample and thermalize in a few seconds via collisions. The thermalized positron directly annihilates with a free electron or forms a system consisting of the electron–positron bound state called positronium (Ps). For low electron density materials such as polymers, positrons have enough time before the annihilation to form the Ps atom. Depending on the mutual spin orientation of the positron and electron, Ps exists in two states, i.e., ortho-positronium (o-Ps) with parallel spin and para-positronium (p-Ps) with antiparallel spins. In a vacuum, due to the parity conservation rule, p-Ps self annihilates into two 511 keV gamma with a mean lifetime of about 0.125 ns. For o-Ps, the parity rule forbids two-quantum decay, and annihilation occurs via three quantum emissions with a lifetime of about 142 ns. From the PAS point of view, Ps self-annihilation provides no information about the material. In the presence of the material, due to the charge neutrality of the o-Ps atom, it can pick off an electron of the surrounding atom and decay in two gamma rays. This mechanism leads to a significant decrease in the o-Ps lifetime (2 to 4 ns) and is called pick-off annihilation [13]. Figure 1 shows the different mechanisms of positron annihilation in an oxygen-content polymer.

3. Experimental details

3.1. CDBS technique

CDBS experiment is performed at the Nuclear Science and Technology Research Institute (NSTRI) for four samples, i.e., PP, LDPE, PMMA, and PTFE polymers to explore the sensitivity of the positron to different chemical environments. The characteristics of the investigated polymers are listed in Table I. These polymers have been selected because their characteristic atoms have similar electronic structures ($2s2p$ orbitals), which facilitate the analysis of the results.

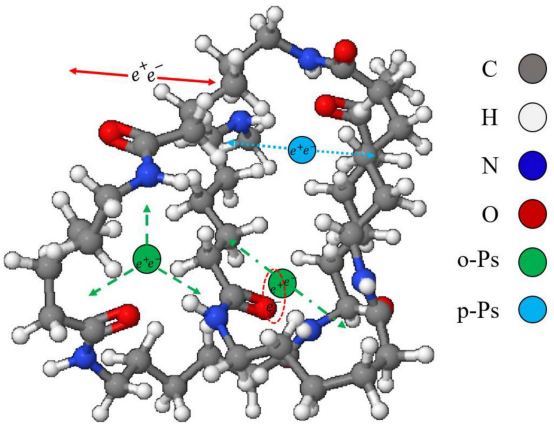

Fig. 1. Different mechanisms of positron annihilation in the investigated sample. Solid red arrows — direct positron annihilation with a free electron. Blue dotted arrows — p-Ps self-annihilation. Green dash arrows — o-Ps undergoing self-annihilation to three photons. Green dash-dotted arrows — o-Ps annihilation via the pick-off mechanism.

TABLE I

The characteristics of the investigated polymers by CDBS technique.

Polymer name	Group	Electronic structure	Density [g/cm^3]
LDPE	hydrocarbon	C: $2s^2 2p^2$	0.930
PP	hydrocarbon	C: $2s^2 2p^2$	0.861
PMMA	oxygen-containing	O: $2s^2 2p^4$	1.159
PTFE	fluorine-containing	F: $2s^2 2p^5$	2.2

The details of our modern 2D-CDBS spectrometer and the applied procedure for calibration, measurement of the long-term stability, energy resolution, and positron source characterization are presented in our previous work [14]. The longitudinal momentum of the annihilated electrons (p_l) is measured using the CDBS spectrometer for each sample. Each experiment lasts 10 days to obtain enough statistics to calculate the contribution of core electrons in annihilation. The competition between different electrons for the annihilation of positrons is described by the orbital electron momentum spectrum (OEMS) [15]. Figure 2 shows the OEMS of the investigated samples. In OEMS, the differences in the low-momentum part of the spectrum are ignored, and the contribution of high-momentum electrons is in focus. The peak at OEMS is a signature of characteristic elements and reflects the chemical environment of annihilation sites. The OEMS of the investigated samples can be described as follows [15]:

- Hydrogen has no core electron, so the peak position at OEMS relates to the positron annihilation with core electrons of either carbon or characteristic atoms of polymers.

- LDPE and PP have the same characteristic atom. So, they have the same peak position and are not distinguishable from each other by OEMS peak position.
- The amounts of positron annihilation by core electrons are reflected in the peak intensity of OEMS. The peak intensity increases by the total number of electrons at $2p$ orbitals of characteristic atoms.
- Due to the existence of polar groups in PTFE (C–F) and PMMA (C=O), the negative charges of the polar groups trap the positrons and facilitate direct positron annihilation by core electrons of the characteristic atoms.

3.2. PALS technique

The PALS experiment is performed for seven samples with a different atomic concentrations of oxygen, i.e., nylon-6, PMMA, PVA, PEO, PEG, PVAC, and PET. The LDPE (with no oxygen in the content) is also selected as the reference. Figure 3 shows the configuration of our recently developed digital PALS spectrometer. This spectrometer is based on a CAEN waveform digitizer (DT5730B) that samples directly at the anode signals of two face-to-face plastic scintillators. In this work, we used the Nyquist sampling theorem [16] for digital spline interpolation of the anode signals because the valuable information at the rise time of the signal may be lost due to the low sampling rate of our digitizer (500 MHz).

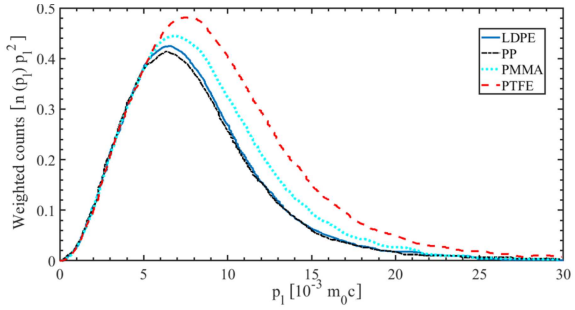

Fig. 2. The measured OEMS for the investigated polymers [15].

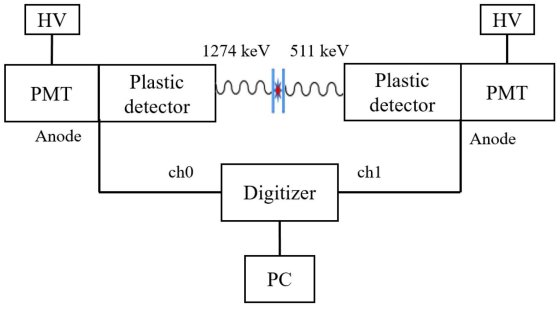

Fig. 3. Configuration of the PALS spectrometer based on waveform digitizer.

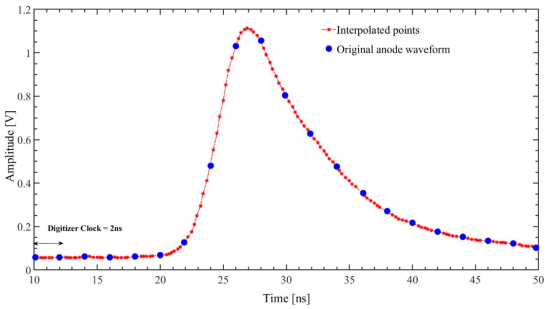

Fig. 4. The interpolated signal for $N = 7$ points between the original anode waveform signals.

The Nyquist theorem is a fundamental tool that allows us to record the time stamp below the clock of the digitizer. The anode signals with a sampling time of 2 ns can be reconstructed by convolving the signal with a sinc function to achieve the time stamp of about a few ps using

$$g(t) = g_s(t)\mathrm{sinc}(t) = \sum_{i=1}^{+\infty} g_s(i)\,\mathrm{sinc}\left(\frac{t - i\,\Delta T}{\Delta T}\right), \tag{1}$$

where $g_s(i)$ is the i-th sample of an anode signal, ΔT is the sampling time (2 ns in our case), and the sinc function is used for normalization and is defined as

$$\mathrm{sinc}\,(x) := \frac{\sin(\pi x)}{\pi x}. \tag{2}$$

Using (1), we can simply divide the time interval between two consecutive samples (j and $j+1$) into N parts to obtain the k-th interpolated value $F(j,k)$ by

$$F(j,k) = \sum_{i=1}^{+\infty} g_s(i)\,\mathrm{sinc}\left(j, \frac{k}{N} - i\right) = \sum_{i=1}^{+\infty} g_s(j-i)\,\mathrm{sinc}\left(i + \frac{k}{N}\right). \tag{3}$$

The raw waveform was recorded in a binary file using the CoMPASS software provided by CAEN Company [17]. Using (3), the original anode signal given in Fig. 3 was redrawn to obtain the interpolated points. Figure 4 shows a typical interpolated signal for $N = 7$ points between two original sampled points.

The finest technique for time pick-off is constant fraction discrimination (CFD). The CFD method has been recognized during the minimization procedure of the time jitter in leading-edge timing measurement [18]. The CFD algorithm measures the time when the sampled signal value reaches a fixed fraction of the pulse height. Triggering the constant fraction of the anode signal can reduce the amplitude walk issue, which often appears in the leading edge technique. Moreover, a simple linear interpolation between two points can solve the problem of sampling frequency and improve the time resolution

TABLE II

Results of the PALS technique.

Sample	Oxygen concentration [% atomic]	τ_1 [ns]	I_1 [%]	τ_2 [ns]	I_2 [%]	τ_3 [ns]	I_3 [%]	χ^2
LDPE	0	0.223 ± 0.014	44.57 ± 0.84	0.489 ± 0.031	24.80 ± 0.38	2.67 ± 0.08	30.63 ± 0.19	1.14
Nylon-6	5	0.216 ± 0.007	47.24 ± 0.76	0.466 ± 0.022	34.57 ± 0.17	2.44 ± 0.10	18.19 ± 0.79	0.99
PMMA	13.33	0.243 ± 0.023	51.36 ± 0.97	$0.451 \pm .017$	31.69 ± 0.08	2.97 ± 0.09	16.95 ± 0.85	0.98
PVA	14.28	0.287 ± 0.003	56.07 ± 0.12	0.472 ± 0.021	32.24 ± 0.12	2.17 ± 0.02	11.69 ± 0.69	1.05
PEO	14.28	0.232 ± 0.019	55.91 ± 1.21	0.457 ± 0.019	30.65 ± 0.16	2.09 ± 0.06	13.44 ± 0.72	1.17
PEG	16.16	0.251 ± 0.027	54.75 ± 1.02	0.491 ± 0.028	30.94 ± 0.44	2.16 ± 0.08	14.31 ± 0.35	0.97
PVAC	16.6	0.241 ± 0.035	54.08 ± 0.37	0.432 ± 0.037	31.25 ± 0.19	2.05 ± 0.13	14.67 ± 0.23	1.23
PET	18.18	0.252 ± 0.002	53.65 ± 1.07	0.479 ± 0.063	33.41 ± 0.41	2.08 ± 0.09	12.94 ± 0.38	1.17

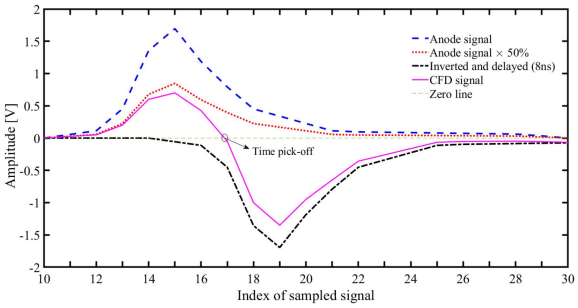

Fig. 5. The generated CFD signal using a typical interpolated anode signal.

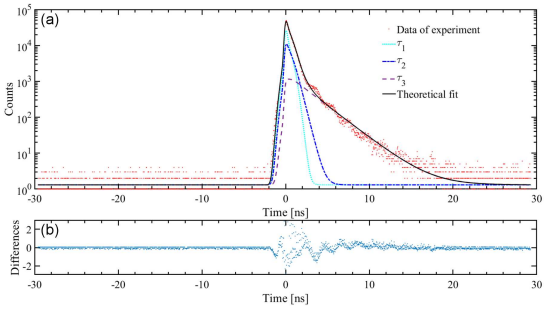

Fig. 6. The PALS spectrum of nylon-6 sample fitted by three discrete exponentials (a) and the residual differences between data points and theoretical fit (b).

of the spectrometer. After the digital interpolation of the anode signal, the CFD is calculated for the n-interpolated anode signal $V(n)$ using

$$\mathrm{CFD}(n) = F\,V(n) - V(n - \Delta), \tag{4}$$

where F is the CFD fraction and Δ is the time delay of CFD. Finally, the intersection of the CFD signal by $y = 0$ (CFD zero-cross) determines the time stamp of the event. Figure 5 shows a typical generated CFD signal using the interpolated anode signal.

The optimum value of F depends on the timing characteristic of the plastic scintillator and its PMT. The parameters F and Δ in (4) should be optimized to obtain the best timing resolution. We measured the FWHM of the ^{60}Co for different values of CFD fractions and delay. The optimum time spectrum of the correlated gamma of ^{60}Co (1173 and 1332 keV) was obtained at $F = 50\%$ and $\Delta = 4$ ns. Assuming that the timing distribution of the coincident events follows a Gaussian distribution, the FWHM of the fitted Gaussian is calculated 173 ps.

Using the mentioned setup, the coincidence count rate is about 35 counts/s for a 1 MBq ^{22}Na source. Figure 6 shows the PALS spectrum measured for the nylon-6 sample decomposed to three discrete exponentials using LT-10 software [19]. The shortest lifetime (τ_1) and its related intensity (I_1) are characteristics of p-Ps self-annihilation and do not matter in our investigation. The medium lifetime (τ_2) originates from the positrons that directly annihilate at the network flaws of the polymers. The longest-lived component ($\tau_3 \simeq 2$–3 ns) is attributed to the o-Ps annihilation in the sample that is influenced by the chemical environment of the annihilation sites. The results of the PALS experiment for all the investigated samples are listed in Table II.

4. Discussion on results

According to the results of the PALS experiment presented in Table II, the longest lifetime ($\tau_3 \simeq 2$–3 ns) and its intensity (I_3) are related to the o-Ps atom annihilation modified by the pick-off mechanism. The comparison of I_3 and τ_3 parameters for the LDPE sample (no oxygen) and nylon-6 (5 atomic percent of oxygen) shows a 40% decrease in I_3 and a 9% decrease in τ_3 parameters. Although a general comparison of the LDPE sample with other oxygen-containing samples confirms a nonlinear reduction of the o-Ps intensity and lifetime, this conclusion is not correct for the PMMA sample. For the PMMA, although the intensity of o-Ps is decreased, its lifetime is increased compared to the LDPE sample. To ensure the accuracy of the measurement, this sample was tested again, and

a similar result was obtained. However, the study of the results presented by Yang et al. [20] also shows that the PMMA ($\tau_3 = 2.09$ ns) has a higher lifetime than the PEEK ($\tau_3 = 1.82$ ns) with a lower oxygen concentration (8.8%) [20]. Considering that among the measured polymers, PMMA is the only polymer that is completely amorphous, this contradictory behavior seems to be related to the trapping of o-Ps atoms in the elementary free volumes of the sample. An important question that should be addressed is which factor leads to the decrease in the lifetime and intensity of o-Ps for the oxygen-containing samples.

From the PAS point of view, the Ps atom can interact with oxygen in two ways:

1. Electron sharing and conversion to free positron according to

$$\mathrm{Ps} + \mathrm{O_2} \rightarrow \mathrm{e^+} + \mathrm{O_2}. \tag{5}$$

2 Conversion of the o-Ps atom to p-Ps in the presence of oxygen according to

$$\text{o-Ps} + \mathrm{O_2} \rightarrow (\text{Ps-O}_2)^* \rightarrow \text{p-Ps} + \mathrm{O_2}, \tag{6}$$

where the unpaired electrons in the oxygen atoms enhance the Ps annihilation via the electron exchange mechanism [21].

Both the mentioned mechanism leads to a decrease in the positron lifetime and, consequently, the recorded intensity of o-Ps decreases. A general comparison of the PALS results for nylon-6 with the other samples again confirms the quenching role of the oxygen atom in the o-Ps formation. However, for the PVA, PEO, PVAc, and PET, where the differences in the oxygen concentration are around 4%, no specific behavior was seen in the I_3 and τ_3 parameters. It seems that in this range of differences, the defect size, crystallinity, density, and bond types (C = O or C–O) determine how the I_3 and τ_3 parameters change with the oxygen concentration.

5. Conclusion

In this paper, the oxygen sensing ability of the PAS technique for Ps imaging was investigated. To conduct the experiments, the first PALS spectrometer based on digital pulse processing has been designed, commissioned, and optimized in the country. This spectrometer makes it possible to record the time difference of events with a channel width of 2 ps and a timing resolution of 173 ps using plastic scintillation detectors. To determine the sensitivity of the technique to the presence of the polar groups with carbon-oxygen bonding, 4 polymer samples were measured using 2D-CDBS techniques. The results of this investigation confirmed that the OEMS obtained by the Doppler broadening experiment is sensitive to the presence of oxygen in the polymers. To determine the parameters related to the amount of oxygen in the PALS technique, 7 tissue-equivalent polymers with different concentrations of oxygen were investigated by PALS. The results of the PALS experiment confirmed that, in general, as the oxygen concentration in the sample increases, the Ps formation decreases significantly. However, for the samples with a little change in the oxygen concentration, the description of the results needs a series of systematic experiments. The results of this work can significantly contribute to the development and translation of the Ps imaging into clinical applications for in-vivo assessment of the degree of hypoxia which has been described in [22]. The ongoing investigations aim at the advent of a total-body PET system for the detection of pathologies on a molecular level in the whole patient body before the structural abnormalities [23]. Further to this work, we are going to commission an age-momentum annihilation spectrometer to identify the effective parameters of the Ps annihilation in tissue equivalent samples.

Acknowledgments

The authors would like to gratefully acknowledge the financial support of the Jagiellonian University for the attendance at the 4th Jagiellonian Symposium on Advances in Particle Physics and Medicine, 10–15 July 2022, Krakow, Poland.

References

[1] R.W. Siegel, *Annu. Rev. Mater. Sci.* **10**, 393 (1980).

[2] A. Biganeh, O. Kakuee, H. Rafi-Kheiri, *Appl. Radiat. Isot.* **166**, 109330 (2020).

[3] P. Moskal, B. Jasińska, E. Stępień, S.D. Bass, *Nat. Rev. Phys.* **9**, 527 (2019).

[4] H. Michael, P. Vaupel, *J. Natl. Cancer Inst.* **93**, 226 (2001).

[5] P. Moskal, *IEEE Nuclear Science Symposium and Medical Imaging Conf. (NSS/MIC)*, IEEE, 2019.

[6] P. Moskal, D. Kisielewska, C. Curceanu et al., *Phys. Med. Biol.* **64**, 5 (2019).

[7] P. Moskal, K. Dulski, N. Chug et al., *Sci. Adv.* **7**, 42 (2021).

[8] P. Moskal, A. Gajos, M. Mohammed, J. Chhokar, N. Chug, C. Curceanu, W. Wiślicki, *Nat. Commun.* **12**, 1 (2021).

[9] E. Stepien, E. Kubicz, G. Grudzien, K. Dulski, B. Leszczynski, P. Moskal, *Eur. Heart J.* **42**, 1 (2021).

[10] P. Stepanov, F. Selim, S.V. Stepanov, A. Bokov, O. Ilyukhina, G. Duplâtre, V. Byakov, *Phys. Chem. Chem. Phys.* **22**, 5123 (2020).

[11] Petr Stepanov, RooPositron Github repository.

[12] K. Shibuya, H.Saito, F. Nishikido, M. Takahashi, T. Yamaya, *Commun. Phys.* **3**, 173 (2020).

[13] Y. Kobayashi, K. Haraya, S. Hattori, T. Sasuga, *Polymer* **35**, 925 (1994).

[14] A. Biganeh, O. Kakuee, H. Rafi-Kheiri, M. Lamehi-Rachti, *J. Instrum.* **14**, 2017 (2019).

[15] A. Biganeh, O.Kakuee, H. Rafi-Kheiri, M. Lamehi-Rachti, N. Sheikh, E. Yahaghi, *Radiat. Phys. Chem.* **166**, 108461 (2020).

[16] P. Vaidyanathan, *IEEE Trans. Circuits Syst. I* **48**, 1094 (2001).

[17] CAEN Electronic Instrumentation, Compass Multi-Parameter DAQ Software for Physics Applications, revision 2.0.1, 2022.

[18] W. McDonald, D. Gedcke, *Nucl. Instrum. Methods* **55**, 1 (1967).

[19] J. Kansy, *Nucl. Instrum. Methods Phys. Res. A* **374**, 235 (1996).

[20] J. Yang, T. Zhang, L. Han, X. Cao, R. Yu, B. Wang, *Spectrochim. Acta A Mol. Biomol. Spectrosc.* **177**, 97 (2017).

[21] R. Ferrell, *Rev. Mod. Phys.* **28**, 308 (1956).

[22] P. Moskal, E. Stępień, *Bio-Algorithms Med-Syst.* **17**, 311 (2021).

[23] P. Moskal, E. Stępień, *PET Clinics* **15**, 439 (2020).